Force Spectroscopy of Single Biomolecules

Matthias Rief*[a] and Helmut Grubmüller*[b]

Many processes in the body are effected and regulated by highly specialized protein molecules: These molecules certainly deserve the name "biochemical nanomachines". Recent progress in single-molecule experiments and corresponding simulations with supercomputers enable us to watch these "nanomachines" at work, revealing a host of astounding mechanisms. Examples are the fine-tuned movements of the binding pocket of a receptor protein locking into its ligand molecule and the forced unfolding of titin, which acts as a molecular shock absorber to protect muscle cells. At present, we are not capable of designing such high precision machines, but we are beginning to understand their working principles and to simulate and predict their function.

KEYWORDS:

atomic force microscopy · molecular dynamics simulations · molecular recognition · protein folding · single molecules

Introduction

Self-organization is a key feature of biological systems. The variety of specific and tunable interactions between biomolecules has given rise to the formation of complex systems like cells and even whole organisms. The three-dimensional structures of biomolecules on their own, such as the fold of proteins and the RNA structure, are impressive examples of self-organization. More than 13 000 available protein structures demonstrate their complex and, at the same time, highly ordered spatial organization (see the box "Protein Structure"). Understanding these self-organization processes in molecular detail requires precise knowledge on how the involved interactions, like hydrogen bonds, forces between charges, chemical bonds, van der Waals interactions, and so forth, eventually lead to a defined structure. However, little experimental information on these complex energy landscapes is available.

For a long time, experimentalists have been able to measure binding or folding energies of the interactions involved. Ensemble-averaged information can be obtained from calorimetry experiments. However, such experiments do not yield information on the details of the energy landscapes that determine the three-dimensional structure of the biomolecules. The development of scanning probe techniques has enabled us to measure the forces which stabilize biomolecular structure directly on a single molecule. In this article, we would like to demonstrate how information about the underlying energy landscapes can be obtained from such force measurements in a combination of theory and experiment.

Force Spectroscopy

How is it possible to grab single molecules by their ends, subject them to a controlled load, and measure the elastic deformations? The invention of the scanning tunneling microscope by Gerd Binnig and Heinrich Rohrer in 1982 and, later, of the atomic force microscope (AFM) by Calvin Quate supplied us with the tools necessary to accomplish exactly that task. Although these techniques had initially been developed to image surfaces with atomic resolution, researchers soon started to use them for the manipulation of atoms and molecules. The micromachined cantilever spring of the AFM can be used as a pico-Newton force measuring device (Figure 1 a). A piezoelectric actuator allows positioning of the cantilever spring to an accuracy of Ångströms. The deflection of the spring is proportional to the acting force and can be measured to a very high precision using a simple light pointer.

The tip of an AFM cantilever has a radius of approximately 10 nm. Biopolymers typically have a similar size. Thus an AFM tip can pick out single molecules even from a dense layer and mechanical experiments can be performed. Molecular recognition was the first example where this was demonstrated.

Molecular Recognition

Specific binding of a ligand molecule ("key") to a receptor protein ("lock") is a basic working principle of molecular recognition processes in the human body. The immune system tracks down foreign substances by expressing antibodies, which bind specifically to structures on their surface. The communica-

[a] *Dr. M. Rief*
Lehrstuhl für Angewandte Physik, Biophysik und neue Materialien
Ludwig-Maximilians-Universität München
Amalienstrasse 54, 80799 München (Germany)
Fax: (+49) 89-2180-2050
E-mail: Matthias.Rief@physik.uni-muenchen.de

[b] *Dr. H. Grubmüller*
Arbeitsgruppe für Theoretische Molekulare Biophysik
Max-Planck-Institut für biophysikalische Chemie
Am Fassberg 11, 37077 Göttingen (Germany)
Fax: (+49) 551-201-1089
E-mail: hgrubmu@gwdg.de

Protein Structure

Proteins are complex, folded polymers,[1] with the chemical formula H-(NH-HCR-CO)$_n$-OH, consisting of the 20 naturally occurring amino acids; R stands for one of the 20 amino acid residues. The sequence of these residues along the polypeptide chain (primary structure) is determined genetically and determines in turn the three-dimensional structure (tertiary structure) as well as the function of the respective protein.

In contrast to most other polymers, the position of each atom in a protein molecule is exactly defined—sometimes down to fractions of an Ångström—and thus can be determined by X-ray diffraction studies on protein crystals.

Figure a) shows the relatively small protein bovine pancreatic trypsin inhibitor (BPTI), which consists of 58 amino acids. BPTI can block the digestion enzyme trypsin. Except for unpolar hydrogen atoms, all 568 atoms of the molecule are represented as balls with their respective van der Waals radii (carbon gray, oxygen red, nitrogen blue, polar hydrogen atoms white, and sulfur yellow). Figures b) and c) show the same protein in representations that emphasize its chemical structure. In addition, the spatial sequence of the peptide chain is highlighted by rainbow coloring the protein backbone from red via yellow and green to blue. Each of the 58 amino acids of the protein contributes six atoms, -CO-HC$_\alpha$-NH-, to the protein backbone. To each C$_\alpha$ atom, one of the 20 different side groups is attached (like the arginine amino acid in the upper right part of BPTI).

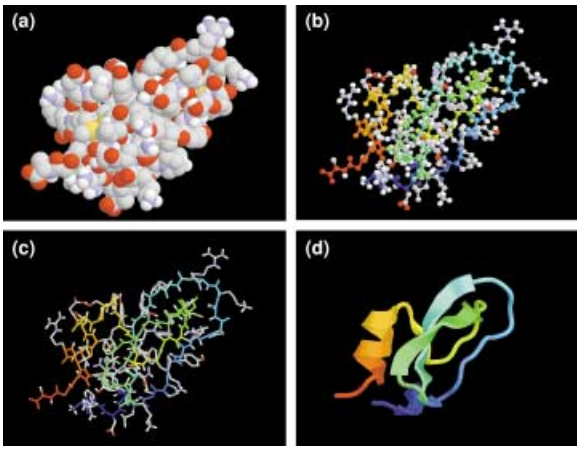

For clarity, and to emphasize the "architecture" of a protein, a simplified "ribbon representation", Figure d), is chosen. Here only the overall fold of the protein backbone is shown, whereas side groups are completely ignored. In addition, the two most common local structural motifs (secondary structure elements) of the peptide chain, α-helices (red/orange) and β-sheets (green/cyan) are represented by coils and arrows. Each of the four representations are based on the same structural model at atomic resolution.

tion of nerve cells also requires neurotransmitters to dock onto their respective receptors on the ion channel to control its activity. Only highly specific interactions can ensure that, in a puzzling variety of signaling substances in the body, each messenger substance can find its correct target. Force is a natural measure for how well the molecules are attached to each other. A cell adhesion molecule, for example, performs its task well if the force required to detach it from its counterpart is high. Many diseases are related to a malfunction of such molecular recognition processes. A detailed understanding of the molecular binding process, together with the information about binding forces, could help to tailor highly specific drugs.

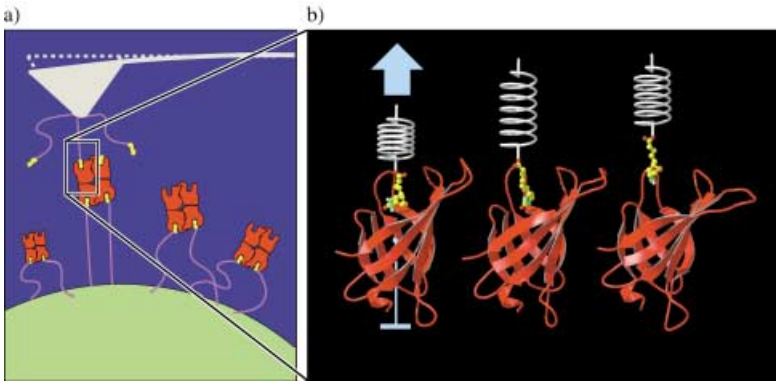

Figure 1. *With an atomic force microscope, single molecules can be subjected to a controlled load and the acting forces can be measured. Ligands (yellow) and receptors (red) are attached to the cantilever tip (gray) and the surface (green) via linker molecules (magenta). Both in the experiment (a) and in the simulation (b), the ligand is subject to an increasing pulling force, and the rupture force is measured.*

Measuring Rupture Forces

In 1994, Ernst-Ludwig Florin, Vincent Moy, and Hermann Gaub succeeded in measuring the binding forces of single molecules for the first time.[2] As a model system, they chose biotin and streptavidin. The structure of these molecules is known to atomic detail, and their binding energy and specificity are extraordinarily high.

As shown in Figure 1 a, single biotin molecules were coupled covalently to an AFM tip via chemical linker molecules. In a similar way, the surface was functionalized with streptavidin molecules. Subsequently, the AFM tip was brought in contact with the surface and a few streptavidin – biotin complexes formed. The tip was then retracted, and the rupture forces measured. Repeating this measurement several hundred times resulted in a distribution of rupture forces with a clear quantization (Figure 2). The maxima of the force histogram (arrows) correspond to the binding force of one, two, and so forth, molecular pairs. The binding force of the streptavidin – biotin pair was thus determined to be 160 pN per binding pair.

This experiment demonstrated that it is indeed possible to measure binding forces between single ligand – receptor complexes. Moreover, it could be shown that the effective length of the ligand – receptor

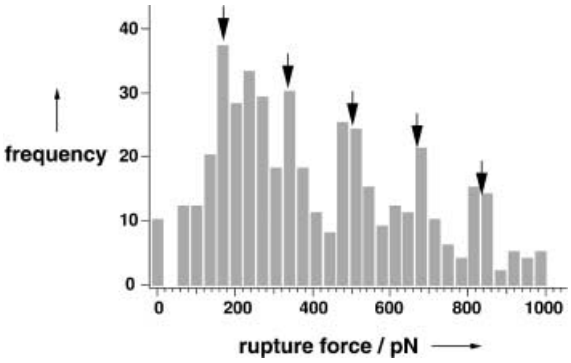

Figure 2. *Distribution of rupture forces of the streptavidin – biotin complex. The arrows mark the observed quantization caused by rupture of one, two, or more, bond pairs.*

bond is approximately 5 Å. This is considerably longer than the bond length of a single hydrogen bond or a van der Waals interaction, which suggested that the measured binding force is the result of many such interactions.

Ligand – Receptor Unbinding Simulations

The details of the bond separation at the atomic scale are not resolved in those measurements. We therefore modeled and simulated, atom by atom, the relevant aspects of the experiment.[3] We employed molecular dynamics simulations (see the box "Molecular Dynamics Simulations"), which are rather accurate but computationally quite intensive. All interatomic forces were included, and the movement of each individual atom was calculated by numerically integrating Newton's equations of motion.

In addition to the interatomic forces, we also had to model the pulling force exerted on the ligand by the retracting AFM tip (Figure 1 b). This was accomplished through a harmonic potential acting on the same atom of the ligand molecule (yellow) that is covalently bound to the linker polymer in the experiment. Like the AFM tip in the experiment, the potential in the simulation was shifted uniformly upwards, while the center of mass of the receptor protein (red) was kept fixed.

The series of three snapshots shows that the biotin molecule is initially (Figure 1 b left) fixed inside the binding pocket of the receptor through a network of interatomic forces (mainly van der Waals contacts and hydrogen bonds). As soon as the pulling force exceeds the sum of these forces, the biotin detaches from the streptavidin in a stepwise manner (Figure 1 b middle). The extension of the spring indicates the required force. Once the complex is separated (Figure 1 b right), the biotin molecule can yield to the tension and the pulling force decreases. The maximum force exerted during this process agrees very well with the measured unbinding forces: We now have a microscopic model of the rather complex reaction path of streptavidin – biotin separation. Such a model can be used to suggest mutants with designed binding properties and forces, which can subsequently be tested experimentally.

Elasticity of Polysaccharides

While the preceding paragraph focussed at the *inter*-molecular binding forces, we now turn to force spectroscopy measurements of the *intra*-molecular forces: Which are the molecular forces that govern the mechanical properties of single polymer molecules? What determines the stability of proteins? The example of polysaccharide elasticity illustrates the interplay of force experiments and simulations.

Polysaccharides play an important role as structural building blocks in plants (as wood for example). A huge part of the global biomass consists of polysaccharides. Polysaccharides consist of many glucose subunits which are linked together (see Figure 3 left). They differ by their linkages: in dextran (above) one glucose monomer is linked by its C_1 carbon atom to the C_6 atom of its

Molecular Dynamics Simulations

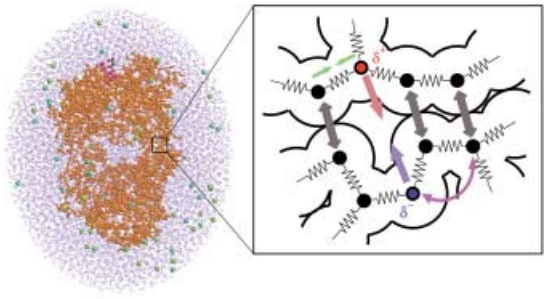

Within a macromolecule (Figure, left, red part), various kinds of interatomic forces act. Forces arising from chemical bonds, here represented as springs, compel bound atoms into their equilibrium distances (green arrows) or equilibrium angles (magenta). Pauli repulsion (gray arrows) prohibits atoms from penetrating through each other. Long-range interactions, particularly Coulomb forces (red, blue) between partially charged atoms (δ^+, δ^-), contribute significantly to the stability of a protein structure. All these forces (and several others) determine the three-dimensional structure of a protein as well as the motion of each individual atom; they are therefore fully included within a molecular dynamics (MD) simulation. The movement of the atoms is calculated in classical approximation by numerical integration of Newton's equations of motion. This approximation holds at room temperature for many processes.

Because the forces change rapidly with the changing atomic positions, all forces have to be repeatedly updated in small time steps (typically 10^{-15} s). Thus, 10^6 such integration steps simulate the movement of all atoms of the simulation system for the short timespan of one nanosecond. To date, this is the typical length of MD simulations, limited by the available computational resources.

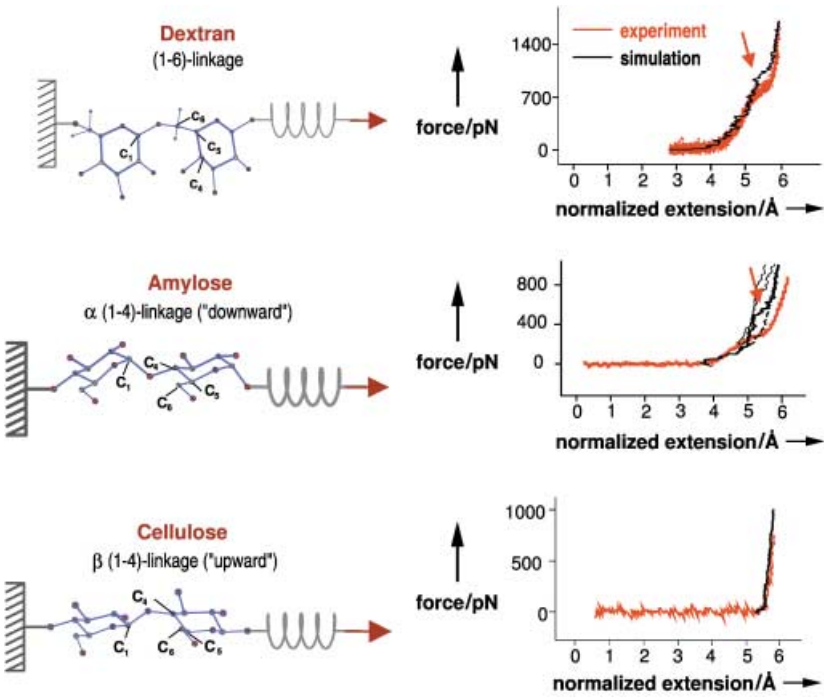

Figure 3. *Left: structures of the polysaccharides dextran, amylose, and cellulose (shown as dimers). To simulate stretching, one end of the polymer is fixed, while the other end is subjected to a harmonic potential (spring) moving in the direction of pulling (arrow). Right: measured (red) and calculated (black) force versus extension curves of the three shown polysaccharides. For amylose, the solid lines show the influence of different side groups; the dotted line shows the elasticity in the absence of side groups.*

neighbor; in amylose (center) and cellulose (below) the linkage is made to the C_4 atom.

In the experiment, the dextran strands are immobilized on a gold substrate and functionalized with receptor molecules, which bind specifically to the ligands attached to the AFM tip (Figure 4).[4] In contrast to the enforced receptor – ligand separation, here we are not interested in the rupture forces but rather in the elastic properties of the dextran polymer. Accordingly, we measure its extension as a function of the applied force.

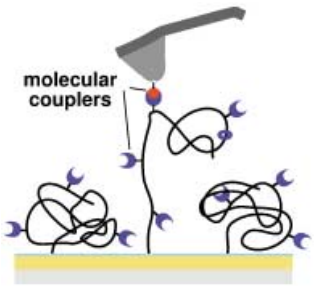

Figure 4. *Measuring intramolecular forces with an AFM. The polymer of interest is linked to the AFM tip through molecular couplers and can be subsequently stretched.*

Figure 3 shows the measured force versus extension traces (red) for three different polysaccharides. The curves for dextran and amylose exhibit a similar pattern. At low force, the elasticity is determined by entropic forces: The restriction of the conformational space of the polymer backbone due to the stretching results in a restoring force even if there are no elastic elements in the chain. Entropic forces are also responsible for rubber elasticity. With greater force, however, the force – extension curve exhibits a characteristic shoulder (arrow): the polymer lengthens without increasing the force. This critical force likely induces an intramolecular structural transition in the polymer, increasing its effective length. Although the difference in the linkage between dextran and amylose may seem subtle, the critical forces of the respective conformational changes differ drastically (700 versus 280 pN). The difference in elastic properties to cellulose is even more surprising: Although chemically identical to amylose and differing only in stereospecificity of the asymmetric C_1 atom, the force – extension trace of cellulose does not exhibit any conformational transition.

Again, molecular dynamics simulations can provide detailed models. In fact, the conformational transition of dextran was first seen in simulations and motivated subsequent experiments.[4] What is the nature of this intramolecular conformational transition? Figure 3, left, shows the set-up of the simulation. Again, the right end of the polymer is subject to a spring potential while the left end is kept fixed. In order to rule out cooperative effects over many monomers, polymers consisting of up to 16 monomers were simulated. For simplicity, only dimers are show in Figure 3.

Force versus extension curves (black) obtained from the simulations are shown in Figure 3, right. In the case of dextran and amylose, as in the experiments, the simulations also show a shoulder indicating a conformational transition. Cellulose, on the other hand, does not exhibit a shoulder, also consistent with the experimental results.

The simulations confirm that intramolecular conformational transitions are responsible for the characteristic shapes (Figure 5). Two different types of transitions can occur. In the case of dextran (left), the monomers change orientation with respect to each other while the rings remain unaffected. For amylose (right), the transition occurs *within* the monomers, and their

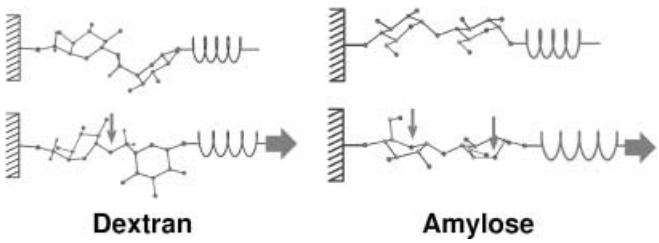

Figure 5. *Force-induced structural changes (arrows) in dextran and amylose. In the relaxed states (above), the sugar monomers adopt the energetically favorable "chair conformation"; when a pulling force is applied (below), the dextran monomers tilt around the polymer axis. In contrast, amylose shows an intramonomeric transition from the "chair" to a "boat" conformation.*

conformation changes. The simulations also explain the different behaviors of amylose and cellulose. Although transitions occur in both amylose and cellulose the associated length change in cellulose is small, such that the transitions do not affect the overall polymer elasticity.

Another interesting effect appeared in amylose. In the experiments, amylose is modified by side groups to ensure solubility of the polymers. These side groups were also included in our simulations. In the absence of side groups, however, the force extension curves change drastically (Figure 3, middle, dotted curve). Here, an inhibitory interaction between neighboring monomers suppresses the transitions almost completely. Moreover, this suggests that relatively minor modifications of the side groups can be used to modulate the elastic properties of amylose significantly (thin lines). Should this turn out to be also true for other polymers, this effect would have significant implications for the material sciences.

Enforced Protein Unfolding

Compared to the stretching of polysaccharides, enforced unfolding of proteins is a much more complex process. The three-dimensional structure of proteins is stabilized by many different and competing interactions (see the box "Protein Structure"). Similar to glasses, the configurational space of proteins exhibits a large number of local energy minima. Thus, a protein requires a timespan from seconds to minutes to find its global free-energy minimum in the course of folding. It is for this reason that the first-principles prediction of three-dimensional protein structures, namely from knowledge of its amino acid sequence only (the "folding problem"), remains one of the key problems in theoretical biophysics. Protein unfolding experiments hold the promise to gain new insights into the protein folding process.

As an example, we chose the muscle protein titin, which is responsible for the passive elasticity of muscle fibers. If a muscle cell is stretched, titin acts as a molecular spring and ensures that the cell relaxes back into its correct shape. Single titin molecules can be extended to more than twice their original length. For a long time, the mechanism of titin elasticity on a molecular level was unclear.

Titin consists of a sequence of more than 200 modules, so-called immunoglobulin domains (Ig domains, Figure 6 a) each consisting of about 90 amino acids, which form a beta barrel (Figure 7, inset 1). Using single-molecule force spectroscopy, we have studied unfolding forces of single titin-Ig domains.[5]

A stretch of eight immunoglobulin domains from human heart muscle was immobilized on a surface and extended in the AFM (Figure 6 a). The pronounced sawtooth pattern reflects the molecular titin elasticity (Figure 6 a, bottom, black curves). Each peak corresponds to the unfolding of a single domain. As soon as the peak force is reached, the domains unfold in an all-or-none process. The distance between two peaks corresponds exactly to the gain in length expected for the 90 amino acids of a domain to completely unfold from a properly folded to a fully stretched polypeptide chain. The rising slopes of each peak reflect the entropic elasticity of the unfolded protein.

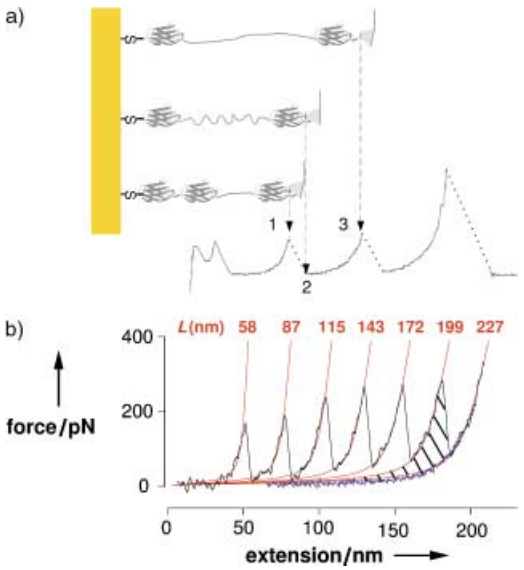

Figure 6. *a) A construct from cardiac titin, consisting of eight immunoglobulin domains (only three shown), was immobilized on a surface and subsequently stretched with an AFM tip. b) Each peak of the force – extension curve corresponds to the unfolding of one single immunoglobulin domain.*

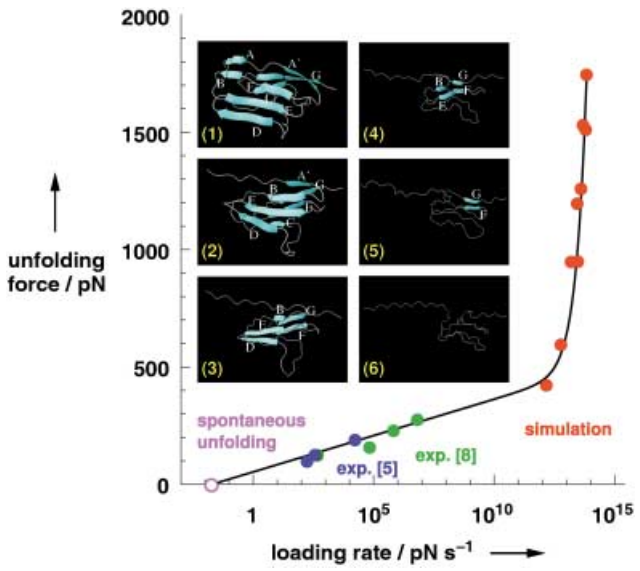

Figure 7. *Measured (blue[5], green[8]) and calculated (red) unfolding forces of titin as a function of the loading rate* kv. *The six insets show snapshots of the protein during simulated unfolding.*

The analysis of the rising slopes (red curves) yields a persistence length—a measure for chain stiffness—of 0.4 nm. Upon relaxation of the unfolded protein chain (blue curve in Figure 6 b), the recorded trace exhibits no discontinuities that would indicate refolding.

It turns out that refolding can happen only against minute forces (<2 pN). Since the blue curve differs from the sawtooth unfolding curve, this experiment is thermodynamically irreversible, and the unfolding process occurs far from equilibrium. Near equilibrium, both unfolding and refolding events should happen with similar force and both curves should exhibit similar

shapes. The large forces required to unfold the titin domains can be explained by the fact that the forced unfolding occurs at nonequilibrium. At equilibrium, the area enclosed by the force–extension curves should be equal to the free energy of folding. However, the mechanically deposited energy per unfolding event (hatched area in Figure 6b, about 1000 k_BT) exceeds the free energy of folding of a single domain (about 10 k_BT) by two orders of magnitude. Thus most of the deposited energy is dissipated. It is this property that makes titin a perfect mechanical shock absorber in muscle. Whenever extreme forces are acting on muscle tissue, a titin domain unfolds before other muscle components are damaged. As soon as tension is relaxed, the unfolded domains will refold. Based on this principle, Paul Hansma (University of California, Santa Barbara, USA) has recently proposed a synthesis of glues which should be able to absorb a lot of energy before detaching.[7]

From the mentioned difference between the folding free energy and the dissipated energy during forced unfolding, another property of the unfolding forces can be readily derived: unfolding forces depend on the pulling velocity. Since under equilibrium conditions the area below the curve has to approach the value of 10 k_BT, the unfolding force has to decrease with decreasing pulling velocity.

A quantitative description of the velocity dependence can be derived from rate theory. Already a simplified picture yields as the most important feature that, to a first approximation, the unfolding force depends logarithmically on the pulling velocity (see the box "Velocity Dependence of Unfolding Forces"). Measurements of titin unfolding for various loading rates were conducted in the group of Julio Fernandez (Mayo Clinic, MN, USA) and by ourselves in Gaub's group (Universität München, Germany).[5, 8] As predicted, the unfolding forces scale to the logarithm of the velocity (Figure 7).

Dynamic Force Spectroscopy

A detailed analysis, as sketched in the last paragraph of the box "Velocity Dependence of Unfolding Forces", predicts deviations from the simple logarithmic dependence. It turns out that these deviations should be determined by the details of the underlying energy landscape. Thus, it should be possible to obtain spatially resolved information on the energy landscape from loading-rate dependent force measurements. This concept is called "dynamic force spectroscopy". Evan Evans (University of British Columbia, Canada) first showed that dynamic force spectroscopy can determine the spatial positions of the energy barriers of the

Velocity Dependence of Unfolding Forces

Consider the blue curve, which describes the free energy $G(x)$ along a reaction coordinate x. Such a reaction coordinate—for example the end-to-end distance of a protein—describes the unfolding of the protein or, alternatively, the unbinding of a ligand from a receptor protein. A barrier separates the folded/bound state (left) from the unfolded/unbound state (right). Actually, such energy landscape is of course much more complex than drawn in this simplified sketch. The following considerations, however, are generally valid for all activated barrier crossing processes, like the enforced unbinding of a ligand–receptor complex and similar single-molecule experiments using "optical tweezers".[6] Through the Boltzmann factor, the barrier height $\Delta G^{\ddagger}$ determines the spontaneous rate of unfolding k_0 and, therefore, the time the protein needs on average to overcome the barrier in a thermally activated process. For titin, this time is approximately an hour. If enforced unfolding was carried out more slowly than this timespan, a zero unfolding force would be measured, because the protein would have unfolded spontaneously already before a considerable force could have been generated.

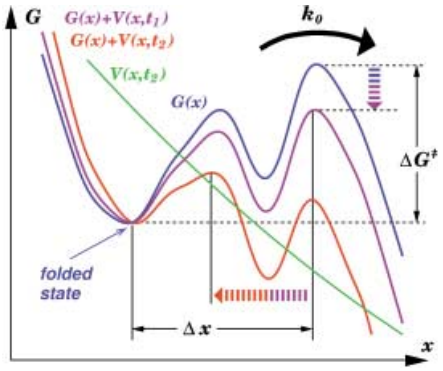

In a similar manner to the setup of the MD enforced unfolding simulations, we describe the pulling force by a time-dependent harmonic potential $V(x,t) = {}^1/_2k(x - vt)^2$ (green), where k is the effective spring constant of the AFM cantilever. Like the piezo stage in the experiment, the minimum of $V(x,t)$ shifts with velocity v. In the case of a soft spring, thermal fluctuations $(k_BT/k)^{1/2}$ are small compared to the rupture length Δx, such that the pulling potential can be approximated by a straight line. Thus, the force $F(t) = kvt$ is constant with respect to x and increases linearly in time with a rate kv.

Accordingly, the applied force deforms the energy landscape (violet, red), such that the barrier height decreases with rate $kv\Delta x$. (The apparent slight shift of the minimum is neglected at this stage.) If the pulling force rises faster than the spontaneous unfolding rate k_0 $(1/\tau = kv\Delta x/\Delta G^{\ddagger} > k_0)$, the protein will unfold as soon as the barrier is low enough to be crossed from thermal excitation within the timescale τ set by the pulling velocity. The unfolding force is then defined as the force acting at this moment. With these assumptions, one can show that the unfolding force $F(kv)$ increases logarithmically with the loading rate kv, namely $F(kv) = (k_BT/\Delta x)\ln(v/k_0\Delta x)$. Note that this result is based on the assumption that the deformation of the energy landscape $G(x)$ by the pulling potential $V(x,t)$ leaves the positions of its minima and maxima unchanged. Clearly, this assumption already breaks down for the depicted case of two energy barriers. Here, above a critical force, the left barrier becomes larger than the right one and thus becomes the global maximum (red curve) and determines the Boltzmann factor. For larger forces, the effective rupture length Δx decreases, and the logarithmic slope increases correspondingly. Thus, the shape of the energy landscape is reflected in the dependence of the rupture force on the loading rate $F(kv)$, that is, in the dynamic force spectrum.

streptavidin – biotin bond with subnanometer resolution without relying on a similar instrumental resolution.[9]

We could take this concept even further and show that by taking into account the continuous shift of each of the barriers with increasing load, the shape of the energy landscape can be reconstructed to a large part. Even the breaking of single hydrogen bonds should be resolvable. The full theory is described in ref. [10].

Protein Unfolding in the Computer

The simple rate theory also allows comparison of experiments and simulation. Recently, the development of powerful parallel computers has allowed the simulation of the complex process of forced protein unfolding. The red data points in Figure 7 show unfolding forces for different loading rates as computed from unfolding simulations. Due to the limited timespan covered by the computationally expensive simulations (10 ns), the chosen loading rates have to be considerably larger than in the experiment. Moreover, beyond 10^{13} pN s^{-1} friction forces contribute with a linearly increasing term γv. This effect can be corrected for, and the logarithmic dependence of the unfolding forces can be derived from the simulations. Accordingly, the solid curve in Figure 7 was obtained by combining the simulation results and the known spontaneous unfolding rate at zero force. Clearly, the calculated curve agrees well with the experimental values, such that our simulations should accurately describe the enforced unfolding process.

Figure 7 shows six snapshots to illustrate the unfolding pathway. The β-strands AB and A′G unfold already very early (1 – 3). Surprisingly, this early unfolding event largely determines the unfolding force. Later stages of the unfolding process (3 – 6) only require smaller forces, and thus cannot be observed in the experiment. Therefore, the effective rupture length of 5 Å is very short, given that the protein is 260 Å longer when completely stretched state as compared to the folded state (see also Figure 6b). Interestingly, in Figure 7 (inset 6), all β-sheets have disappeared although a large part of the protein still has a compact shape. This finding supports the idea that protein folding can be divided into two steps: First, a hydrophobic collapse driven by hydrophobic interactions and, second, a phase of internal reorganization leading to the final protein structure.

These results agree well with simulations by Klaus Schulten and co-workers (University of Illinois at Urbana-Champaign, USA).[11] Based on the central role of β-sheet AB, a mutant has been suggested which was predicted to significantly change the unfolding forces. This prediction was recently confirmed by experiments in Fernandez' group.[12]

The described examples, as well as many others, show that quite often mechanisms and the function of many proteins are to a large extent *mechanical*. With these "machines", nature has built masterpieces of nanotechnology, the mechanical "gears and wheels" of which often consist of only a few atoms. The required energy for ATP synthesis, for example, is transmitted mechanically through a "stalk" that has a diameter of only 1.2 nm. Thanks to the human genome project and other sequencing projects, we now have 10^7 "part lists" (protein sequences) available. Of more than 13 000, we know the three-dimensional structure in atomic detail. To elucidate their working mechanisms is a challenge that requires the combination of many different techniques. A better understanding of these nanomachines will help us to use nature's tricks in nanotechnology. Force microscopy and computer simulations can make important contributions here.

From a more general point of view, a new perspective emerges. Going beyond the thermodynamic ensemble description, single-molecule experiments provide access to the mechanical properties of molecules, often far from equilibrium. Quite similar to the study of mechanical devices with an unknown mechanism or function, we probe the mechanical responses of proteins to external forces to learn about their mechanism at the atomic scale.

In addition to the traditional sequence- and structure-based bioinformatics tools, the accurate simulation of single-molecule experiments provides us with the necessary theoretical insight into the underlying mechanical and dynamical processes. Models of force-induced structural changes at the atomic level can be derived, which can be tested against experiment, and thus allow us to watch single molecules at work.

Further information and publications relating to this article may be found at www.biophysik.physik.uni-muenchen.de and www.mpibpc.gwdg.de/abteilung/071. We are grateful to Holger Wagner for the simulation shown in Figure 7.

[1] C. Branden, J. Tooze, *Introduction to Protein Structure*, Garland, New York, NY, **1991**.
[2] E.-L. Florin, V. T. Moy, H. E. Gaub, *Science* **1994**, *264*, 415.
[3] H. Grubmüller, B. Heymann, P. Tavan, *Science* **1996**, *271*, 997.
[4] M. Rief, F. Oesterhelt, B. Heymann, H. E. Gaub, *Science* **1997**, *275*, 1295.
[5] M. Rief, M. Gautel, F. Oesterhelt, J. M. Fernandez, H. E. Gaub, *Science* **1997**, *276*, 1109.
[6] S. Izrailev, S. Stepaniants, M. Balsera, Y. Oono, K. Schulten, *Biophys. J.* **1997**, *72*, 1568.
[7] B. L. Smith, T. E. Schäffer, M. Viani, J. B. Thompson, N. A. Frederick, J. Kindt, A. Belcher, G. D. Stucky, D. E. Morse, P. K. Hansma, *Nature* **1999**, *399*, 761.
[8] M. Carrion-Vazquez, A. F. Oberhauser, S. B. Fowler, P. E. Marszalek, S. E. Broedel, J. Clarke, J. M. Fernandez, *Proc. Natl. Acad. Sci. USA* **1999**, *96*, 3694.
[9] See also A. Janshoff, C. Steinem, *ChemPhysChem* **2001**, *2*, 577.
[10] B. Heymann, H. Grubmüller, *Phys. Rev. Lett.* **2000**, *84*, 6126.
[11] H. Lu, B. Isralewitz, A. Krammer, V. Vogel, K. Schulten, *Biophys. J.* **1998**, *75*, 662.
[12] P. E. Marszalek, H. Lu, H. Li, M. Carrion-Vazquez, A. F. Oberhauser, K. Schulten, J. M. Fernandez, *Nature* **1999**, *402*, 100.

Received: August 14, 2001 [C284]